NeuroImage 229 (2021) 117735

Contents lists available at ScienceDirect

NeuroImage

journal homepage: www.elsevier.com/locate/neuroimage

Mapping grip force to motor networks

Ladina Weitnauer[a], Stefan Frisch[b,d,e], Lester Melie-Garcia[a], Martin Preisig[f], Matthias L. Schroeter[b], Ines Sajfutdinow[c], Ferath Kherif[a], Bogdan Draganski[a,b,*]

[a] LREN, Department of clinical neurosciences - CHUV, University Lausanne, Switzerland
[b] Max-Planck Institute for Human Brain and Cognitive Sciences, Leipzig, German
[c] Day Clinic for Cognitive Neurology, Universitätsklinikum Leipzig, Leipzig, Germany
[d] Department of Gerontopsychiatry, Psychosomatic Medicine, and Psychotherapy, Pfalzklinikum, Klingenmünster, Germany
[e] Institute of Psychology, Goethe-University, Frankfurt am Main, Germany
[f] Department of psychiatry - CHUV, University Lausanne, Switzerland

ARTICLE INFO

Keywords:
Stroke
Brain lesion
Magnetic resonance imaging
Voxel-based morphometry
Voxel-based quantification
Grip force
Structural covariance
Relaxometry
Multi-parameter mapping

ABSTRACT

Aim: There is ongoing debate about the role of cortical and subcortical brain areas in force modulation. In a whole-brain approach, we sought to investigate the anatomical basis of grip force whilst acknowledging interindividual differences in connectivity patterns. We tested if brain lesion mapping in patients with unilateral motor deficits can inform whole-brain structural connectivity analysis in healthy controls to uncover the networks underlying grip force.

Methods: Using magnetic resonance imaging (MRI) and whole-brain voxel-based morphometry in chronic stroke patients (n=55) and healthy controls (n=67), we identified the brain regions in both grey and white matter significantly associated with grip force strength. The resulting statistical parametric maps (SPMs) provided seed areas for whole-brain structural covariance analysis in a large-scale community dwelling cohort (n=977) that included beyond volume estimates, parameter maps sensitive to myelin, iron and tissue water content.

Results: The SPMs showed symmetrical bilateral clusters of correlation between upper limb motor performance, basal ganglia, posterior insula and cortico-spinal tract. The covariance analysis with the seed areas derived from the SPMs demonstrated a widespread anatomical pattern of brain volume and tissue properties, including both cortical, subcortical nodes of motor networks and sensorimotor areas projections.

Conclusion: We interpret our covariance findings as a biological signature of brain networks implicated in grip force. The data-driven definition of seed areas obtained from chronic stroke patients showed overlapping structural covariance patterns within cortico-subcortical motor networks across different tissue property estimates. This cumulative evidence lends face validity of our findings and their biological plausibility.

1. Introduction

There are still major gaps in our understanding of the relationship between brain structure and function that could help reliably predicting motor outcome after stroke. Historically, modeling of the structure-function relationship has relied on univariate methods under the premises of one-to-one mapping. However, there is broad consensus that these traditional mapping approaches are failing to cope with the overwhelming task complexity of integrating the inherent inter-individual variability in both clinical symptoms and objective measurements of lesion localisation and extent. Resolving these limitations requires novel "out-of-the-box" strategies that challenge previous assumptions about mapping between brain lesions and symptoms (Kherif and Muller, 2020). Most recent analytical approaches allowing to map individuals' symptoms to brain networks rather than specific regions represent a breakthrough in the domain of clinical neuroscience and offer a window of opportunity answering questions about structure - function relationships (Fox, 2018).

Grip force - a paradigmatic case of motor control, has been studied from both behavioural and neuroimaging perspective. Functional magnetic resonance imaging (fMRI) studies demonstrated a widespread network involved in force control consisting of the primary sensorimotor cortex, ventral premotor, inferior parietal areas and cerebellum (Keisker et al., 2009; King et al., 2014). Neuroimaging brought also another level of complexity showing the specific contribution of ipsi- and contra-lateral motor cortex activity to grip force control (Ward et al., 2007). The role of the basal ganglia in grip force strength remains controversial with results pointing towards the involvement of the internal

* Corresponding author at: LREN - Département des Neurosciences Cliniques, CHUV, Université de Lausanne, Mont Paisible 16, 1011 Lausanne, Switzerland.
E-mail address: bogdan.draganski@chuv.ch (B. Draganski).

https://doi.org/10.1016/j.neuroimage.2021.117735
Received 22 October 2020; Received in revised form 30 December 2020; Accepted 4 January 2021
Available online 14 January 2021

Table 1
Demographic and behavioural data of study participants in the brain lesion analysis. Abbreviations: TPS – time post stroke, TIV – total intracranial volume, GF - grip force, R – right, L – left, Pat – patients, Ctr – healthy controls.

	Total	Mean (SD) Age [years]	Mean (SD) TPS [months]	Mean (SD) GF R [N]	Mean (SD) GF L [N]	Mean (SD) GF Ratio
Pat	55	46.7 (13.9)	10.6 (10.8)	27.1 (14.0)	28.5 (15.5)	0.59 (0.41)
Ctr	67	44.3 (11.3)	0 (0)	NA	NA	0.95 (0)
Pat vs. Ctr (t-test)		0.3	6.02E-013	NA	NA	4.35E-011
No paresis pat	7	44.6 (14.3)	10.1 (6.5)	34.0 (14.0)	29.8 (13.9)	0.86 (0.17)
L paresis pat	19	47.4 (13.5)	10.7 (8.5)	34.3 (8.9)	15.8 (14.1)	0.51 (0.51)
R paresis pat	29	46.8 (14.4)	10.6 (13)	20.8 (14.1)	36.5 (10.8)	0.57 (0.36)
L vs. R paresis pat		0.874	0.956	5.89E-003	6.78E-007	0.728
No paresis pat vs. L & R paresis pat (t-test)		0.667	0.913	0.165	0.82	0.06

part of globus pallidus (GPi) and the subthalamic nucleus rather than putamen and caudate (Spraker et al., 2007). Cumulating empirical evidence supports the notion that the cortico-spinal tract also has a unique role in grip force modulation (Ward et al. 2007; Pennati et al. 2020).

Lesion network mapping represents a recently introduced analytical strategy that associates focal lesions with patients' symptoms within networks derived from MRI-based measures of brain connectivity (Fox, 2018). The proposed strategy offers a theoretical framework that accommodates the "degeneracy" hypothesis of "many-to-many" mapping to explain the inter-individual differences in recovery of loss of function (Edelman and Gally, 2001; Noppeney et al., 2004). Through the combination of conventional lesion studies with non-invasive brain imaging, lesion network mapping has proved useful in a plethora of conditions including consciousness (Snider et al., 2020), migraine (Burke et al., 2020), to name but a few. Beyond this, the methodological developments of multi-variate analytical methods – e.g. support-vector machines, applied to anatomical neuroimaging data, showed additional benefit for predicting the outcome in chronic stroke patients with upper limb paresis and identifying brain regions critical for individuals' performance (Rondina et al., 2017).

At its current stage, the structural connectivity measures in the published lesion network mapping literature stem from diffusion tractography estimates, integrated into the so-called brain connectome concept (Fox, 2018). Anatomical covariance was proposed as a complementary method to tractography-based assessment of structural brain networks (for review see Alexander-Bloch, Giedd, et al., 2013). The current view about the underlying biological mechanism is that anatomical covariance networks result partly from the coordinated development within different brain areas (Alexander-Bloch, Raznahan, et al., 2013) and connecting white matter pathways as recently demonstrated in the animal model (Yee et al., 2018).

In this study, we leveraged the 'lesion network mapping' strategy (Fox, 2018) to investigate brain networks underlying grip force strength. In a fully data-driven approach, we correlated individuals' grip force with brain anatomy using voxel-based morphometry and automated lesion detection within the SPM framework (Seghier et al., 2008). We then used the derived statistical parametric maps (SPMs) as seed regions for a whole-brain voxel-based covariance analysis using local volume. In parallel, we have also built and assessed the covariance based on multi-parameter maps sensitive to myelin, iron, and tissue water content (Draganski et al., 2011). We hypothesised that starting from the mechanistic view of localising the relationship between loss of grip force and brain anatomy, we can delineate the full extent of motor networks involved in grip force strength.

2. Materials and methods

2.1. Study participants

2.1.1. Lesion study

For the brain lesion study we analysed MRI data of 55 chronic stroke patients seen at the day-care clinic at the Neurology Department, Max-Planck-Institute for Human Cognition and Behaviour, Leipzig - Germany (20 females, age: mean 46.7 years old(yo), median 50yo, SD 13.9yo) and 67 healthy controls (23 females, age: mean 44.3yo, median 43yo, SD 11.3yo). Patients behaviour was assessed using standard testing batteries whilst the clinical details were completed from the medical records. For a summary of demographic and behavioural data see Table 1. The variable "paresis" was assessed in a binary way through neurological examination without rating the severity of motor impairment. Maximum grip force strength of both hands was assessed only in patients using a Seahan Hydraulic Hand Dynamometer (SH5001). For group-level comparisons we used the ratio left to right hand grip force strength. For the healthy controls we considered a ratio of 0.95 based on previous findings (Günther et al., 2008). All participants gave written informed consent prior to study participation. The study was approved by the Ethical Comission of the Medical Departement of the University of Leipzig, Germany.

Table 2
Demographic data of participants in the structural covariance analysis.

	Total	Mean (SD) Age [years]	Mean (SD) TIV [l]
	977	52.0 (16.0)	1.573 (0.161)
Women	487	53.0 (15.6)	1.483 (0.130)
Men	490	51.0 (16.3)	1.663 (0.137)
T-test (women vs. men)		0.053	3.68E-81

2.1.2. Covariance study

For the anatomical covariance study, we used brain MRI data from 977 individuals (487 females, age: mean 52yo, median 53.8yo, SD 16yo) acquired in the context of the CoLaus|PsyColaus community dwelling cohort (Firmann et al., 2008; Preisig et al., 2009). Participants were only included if the medical history and MRI scan had no signs of brain or systemic pathology (see Table 2). All participants gave written informed consent prior to study participation. The study was approved by the Ethical Comission of the Canton of Vaud, Switzerland.

2.2. MRI data acquisition and pre-processing

For the brain lesion study we analyse MRI data acquired on a 3T Siemens Trio (Siemens Medical Systems, Germany) scanner using a T1-weighted (T1w) protocol in sagittal mode using a 3D Magnetization Prepared Rapid Gradient Echo (MPRAGE) sequence (TR = 11.4 ms, TE = 4.4 ms, FoV = 269 mm, flip angle = 30°, 176 contiguous slices, voxel size: 1 × 1 × 1 mm, matrix size = 256 × 256).

For the covariance study, the community dwelling cohort data acquisition was performed on a 3T Siemens Magnetom Prisma (Siemens Medical Systems, Germany) using a 64-channel RF receive head coil and body coil for transmission. The quantitative MRI (qMRI) protocol consisted of three whole-brain multi-echo 3D fast low angle shot (FLASH) acquisitions with predominantly magnetization transfer-weighted (MTw: TR/α = 24.5ms/6°), proton density-weighted (PDw: TR/α = 24.5ms/6°) and T1-weighted (T1w: 24.5ms/21°) contrast with 176 contiguous

slices, voxel size: 1 × 1 × 1 mm, matrix size = 256 × 256 (Helms et al., 2008, 2009; Weiskopf et al., 2013).

Visual inspection of study participant data confirmed an absence of neither macroscopic brain abnormalities nor obvious vascular pathology. The multi-parameter-mapping (MPM) data for all subjects included in the study underwent an automatic quality assessment procedure based on R2* signal homogeneity in the white matter (WM) (Castella et al., 2018). T1w data were visually inspected for abnormalities beyond the cerebral lesions.

2.2.1. Voxel-based morphometry (VBM) and automated lesion detection

For feature extraction from T1w data, we use the "unified segmentation" of Statistical Parametric Mapping and enhanced tissue priors (Lorio et al., 2016) running under Matlab 7.11 (Mathworks, Sherborn, MA, USA). Automated tissue classification resulted in whole-brain probability maps of grey matter, white matter, cerebrospinal fluid, and non-brain tissue. The probability maps were embedded in the outlier-detection framework for automated lesion detection (Seghier et al., 2008). The next step consisted of diffeomorphic registration to Montreal Neurological Institute (MNI) space using the DARTEL toolbox (Ashburner, 2007) that provided spatial registration parameters based on a study-specific template. For VBM analysis the spatial registration procedure included scaling the grey and white matter tissue probability maps by the Jacobian determinants of the deformation field (i.e. "modulation") followed by spatial smoothing with an isotropic Gaussian smoothing kernel of 8 mm full-width-at-half-maximum (FWHM).

2.2.2. Voxel-based quantification (VBQ)

We used the previously described method (Draganski et al., 2011) implemented in an in-house software running under SPM12 to calculate the multi-parameter maps. These included transverse relaxation - R2* maps, magnetization transfer (MT) saturation maps, and proton density maps (PD). The R2* maps were calculated from the regression of the log-signal of the eight PD-weighted echoes. The MT and R1 maps were computed as described in (Helms et al., 2008), using the MTw, PDw and T1w images averaged across all echoes. The PD maps were corrected for local radiofrequency (RF) transmit field inhomogeneities using the B1+ maps computed from the 3D EPI data (Helms et al., 2008) and for imperfect RF spoiling using the approach described by (Preibisch & Deichmann, 2009). The output of this step provides synthetic parameter maps indicative for myelin (MT saturation), iron (R2*), and tissue water (PD*).

2.3. Statistical analysis

The statistical analysis of the two data sets – T1w data from stroke patients and controls, and multi-parameter MRI from the large-scale community dwelling individuals consisted of two separate steps. The first step included a voxel-based implementation of a lesion-symptom mapping that correlated hand grip force across either the lesion tissue class, grey matter or white matter. In a second step, the 1st eigenvariates of voxel values within the resulting statistical parametric maps (SPMs) were used as regressors for the covariance analysis across the whole brain – both within grey and white matter after excluding the seed areas from the search volume (see Fig. 1).

2.3.1. Brain lesion-symptom mapping

We used ANOVA to test at the voxel level for significance and the direction of the gradient between grey, white matter and lesion maps and individual performance in the hand grip task. The corresponding factorial design has one factor with four levels – STROKE w/o PARESIS, LEFT SIDE PARESIS, RIGHT SIDE PARESIS, NO STROKE. We included in the final model the individual hand grip force ratio as interaction term with the group factor. Age, sex, time-since-stroke (TSS), and total-intracranial-volume (TIV) were additional regressors aiming to control for their global effects on brain anatomy.

2.3.2. Structural covariance analysis

In the community dwelling cohort, we extracted the principal eigenvariate of the volume maps (for VBM) and tissue property parameters (for VBQ) from a sphere of 3mm around the peak T-value SPMs obtained from the lesion-based analysis in the first step. The eigenvariates were then used as variables in a multiple regression model including all individuals from the community dwelling cohort. Given the probability of spurious negative correlations in the case of adjustment for global effects – e.g. total intracranial volume (TIV) (Carbonell et al., 2014), we estimate only positive correlations between the eigenvariates and the rest of voxels within brains' grey or white matter (Fig. 1). In all statistical models, we include age, age^2, gender, TIV, and additionally individuals' estimates of tissue class specific volume or the corresponding tissue property parameters assuming a multiplicative global effect (see Taubert et al. 2020). For all analyses, we report results at $p < 0.05$ after family-wise error (FWE) correction for multiple comparisons across the GM or WM compartment or as trends at $p < 0.001$ uncorrected for multiple comparisons.

3. Results

3.1. Brain lesion-symptom mapping

In the whole-brain correlation analysis between the ratio of hand grip force and the lesion probability maps, we found a negative correlation with a homogeneous bilateral cluster comprising basal ganglia and the internal capsule. The very same analysis of grey matter volume maps showed a positive correlation with the caudate and the posterior insula bilaterally. In the white matter analysis, we observed a positive correlation between the ratio of hand grip force and cortico-spinal tract volume in the internal capsule (see Table 3).

3.2. Covariance analysis

Using the brain lesion data-driven definition of seeds for the structural covariance analysis we observed largely overlapping patterns including cortical and subcortical nodes of the motor networks. This was the case not only for morphometry patterns in the VBM analysis, but also for myelin, iron, and tissue water covarying with the rest of the brain in the VBQ analysis.

3.2.1. Cortico-spinal tract seeds

The VBM analysis showed covariance pattern between the seeds' and the volume of the entire intracerebral portion of the cortico-spinal tract bilaterally. For GM, we found covariance with the precentral gyrus, putamen, substantia nigra, and cerebellum volume bilaterally (see Fig. 2).

The analysis of MT maps of the WM demonstrated a pattern accentuated along the cortico-spinal tract bilaterally. For the GM, we observed significant covariance with the precentral gyrus, middle cingulate gyrus, parietal operculum, caudate, thalamus and substantia nigra bilaterally. The analysis of WM R2* demonstrated covariance with the cortico-spinal tract bilaterally and corpus callosum, whilst for GM we report a covariance with the middle cingulate gyrus, caudate, posterior insula, and bilateral thalamus bilaterally. For PD* WM we report covariance along the cortico-spinal tract and in GM – with areas including the postcentral gyrus, the medial segment of the precentral gyrus, occipital pole and hippocampus bilaterally, additionally to the left calcarine cortex, right cuneus, left transverse temporal gyrus, right posterior insula, and right putamen.

3.2.2. Basal ganglia and insula seeds

The VBM analysis in the WM showed covariance between the seed volume and the anterior limb of the internal capsule and the left cortico-spinal tract, whilst in the GM the covariance was restricted to the basal ganglia and thalamus (see Fig. 3). MT of the seeds covaried in the GM

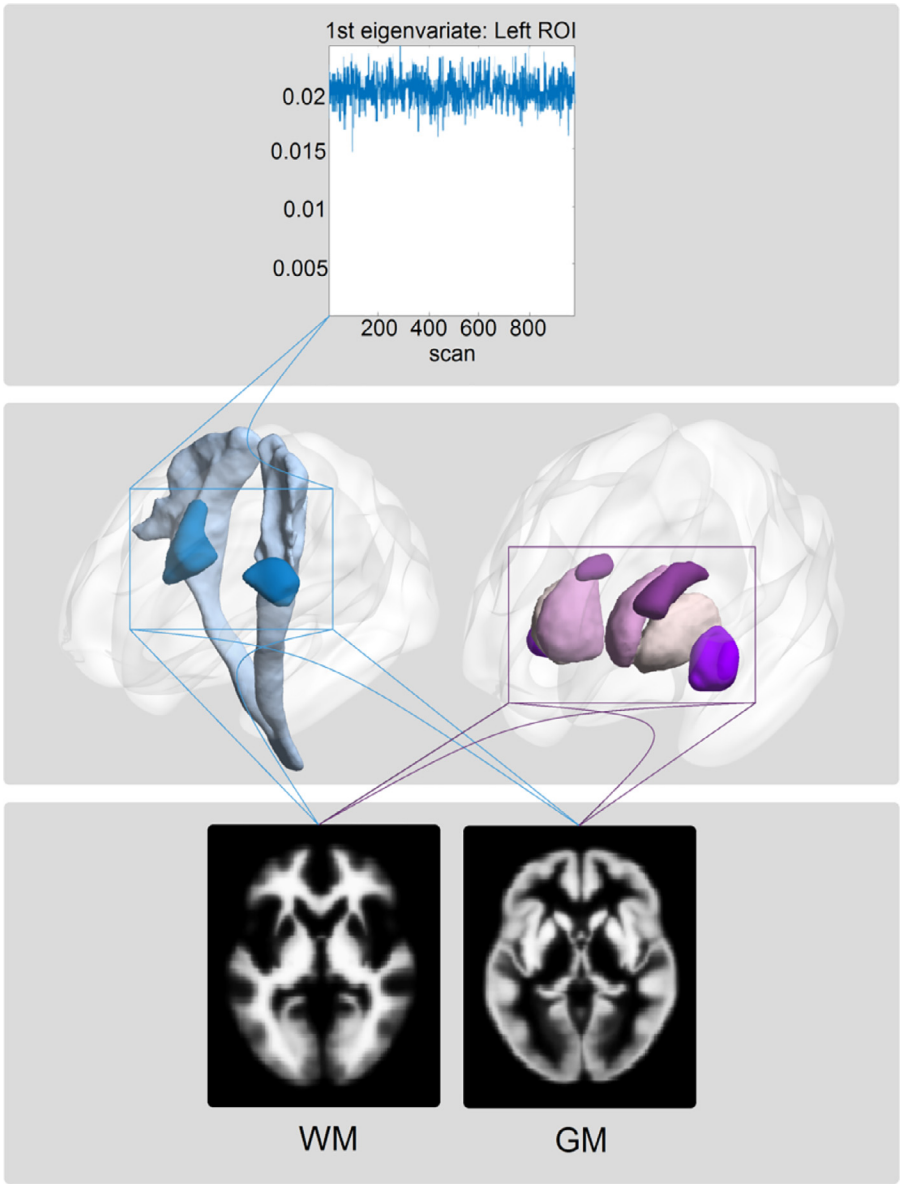

Fig. 1. Schematic representation of the basic principles of structural covariance analysis. *Upper panel*: graphical representation of signal extracted from a statistical parametric map (SPM) of the lesion data analysis. *Middle panel*: localisation of SPM-defined seed regions. *Left*: WM seed (blue) within the cortico-spinal tract. *Right*: GM seeds (violet and purple) within the basal ganglia. *Lower panel*: The extracted principal eigenvariates of the seeds' signal are tested for covariance with the rest of the brain in both white matter (WM) and grey matter (GM) . (For interpretation of the references to color in the text, the reader is referred to the web version of this article.)

Table 3
Peak clusters of the brain lesion-symptom mapping in grey and white matter and lesion volume. Region labelling was done with the Neuromorphometrics toolbox implemented in SPM12b. The statistical threshold is p<0.05 FWE-corrected. LP stands for "left hemiparesis", RP stands for "right hemiparesis". CST stands for "cortico-spinal tract".

	Anatomical region	MNI-coordinates			z-score	t-value
		x	y	z		
VBM, lesion areas						
t-(Ratio_LP_RP)	R CST	24	−12	20	6.55	7.26
	L CST	−23	−17	23	7.53	8.63
VBM, grey matter						
t+(Ratio_LP_RP)	L caudate	−20	−17	23	6.91	7.74
	L insula	−35	−9	−9	5.87	6.37
	R insula	41	−2	−5	5.25	5.61
	R caudate	20	−6	23	4.89	5.18
VBM, white matter						
t+(Ratio_LP_RP)	L CST	−20	−15	23	6.84	7.65
	R CST	21	−9	24	6.51	7.21

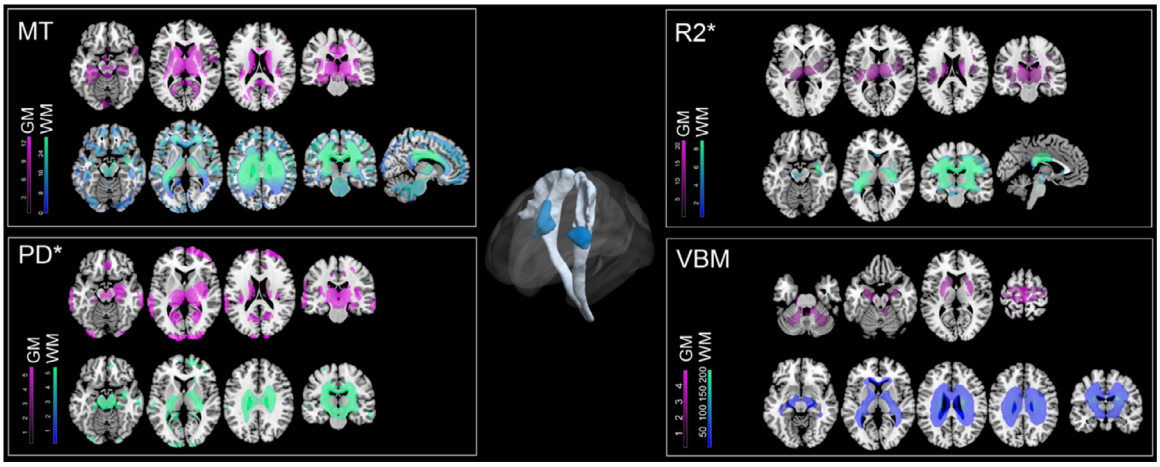

Fig. 2. Statistical parametric maps (SPMs) of the covariance analysis – seeds in the cortico-spinal tract. Covariance maps of local MT (top left), PD* (bottom left), R2* (top right), and volume (bottom right) estimates in the seeds (middle) superimposed on an average MT map in standard MNI space. Colour bar with t-scores for WM (turquoise) and GM (lilac). Results displayed at the statistical threshold of $p<0.05$ FWE-corrected. (For interpretation of the references to color in the text, the reader is referred to the web version of this article.)

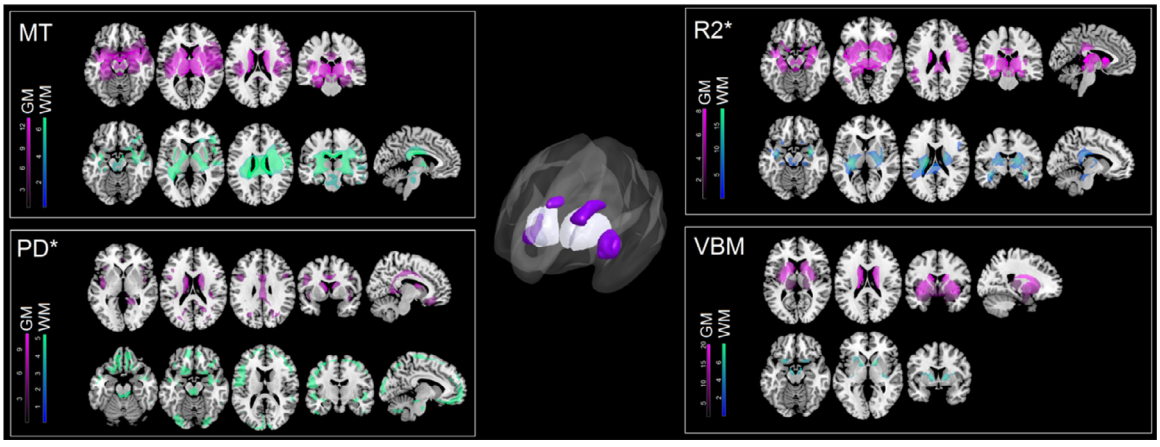

Fig. 3. Statistical parametric maps (SPMs) of the covariance analysis – seeds in the basal ganglia and posterior insula. Covariance maps of local MT (top left), PD (bottom left), R2* (top right) and volume (bottom right) estimates in the seeds (middle) superimposed on average MT map in standard MNI space. Colour bar with t-scores for WM (turquoise) and GM (lilac). Results at statistical threshold of $p<0.05$ FWE-corrected. (For interpretation of the references to color in the text, the reader is referred to the web version of this article.)

with the middle cingulate gyrus, substantia nigra, thalamus and parahippocampal gyrus bilaterally, additionally to the right precentral gyrus. The MT covariance in WM areas was confined to the cortico-spinal tract, fornix bilaterally and corpus callosum. In the GM R2* maps analysis we observed covariance with putamen, thalamus, substantia nigra, middle cingulate gyrus, dentate nucleus bilaterally, the right inferior frontal gyrus and the left parietal operculum.

In WM we show R2* covariance with cortico-spinal tract bilaterally and splenium of the corpus callosum. The PD* maps covariance GM analysis demonstrated the anterior and middle cingulate gyrus, precuneus and the opercular gyrus rectus bilaterally and the left central operculum.

4. Discussion

Our study demonstrates the spatial extent and underlying brain tissue properties of motor networks associated with grip force strength. Rather than making an arbitrary choice between cortical and subcortical seed areas for the structural covariance analysis, we make an informed decision based on lesion mapping of individuals' grip force in chronic stroke patients. We show that the spatial extent of motor networks defined in a covariance analysis largely overlaps between both grey and white matter seeds. The discovered motor network includes cortico-spinal tract, basal ganglia, thalamus, sensorimotor cortex and cerebellum. We not only show the feasibility of structural covariance analysis to uncover brain networks related to motor control, but we also provide information about morphometry and brain tissue properties of the circuitry constituting nodes.

The study's main finding is the discovery of overlapping structural covariance networks associated with grey and white matter nodes implicated in grip force strength. The observation that basal ganglia and cortico-spinal tract sections, determined in the lesion analysis, relate to motor control, corroborate previous findings (Christopher et al., 2014; Prodoehl et al., 2009; Sterr et al., 2014). The spatial overlap between the networks covarying with grey and white matter seeds provides empirical evidence and face validity to our interpretation of unique cortico-subcortical network including basal ganglia, sensorimotor cortex and corresponding white matter tracts. The similarities are not restricted to single anatomical feature, they show substantial consistency across maps indicative for myelin, iron, brain tissue water content beyond the established morphometric estimates. This interpretation is supported by previous findings, showing robust covariance patterns of shared tissue properties in basal ganglia (Accolla et al., 2014) and co-localisation of volume and tissue property effects of ageing (Taubert et al., 2020).

Despite the similarities in the spatial extent of structural covariance networks determined by white and grey matter seeds, we denote at the descriptive level some unexpected differences. Whilst basal ganglia seeds show mainly a subcortical network across anatomical features, the cortico-spinal tract seeds strongly covary with primary sensorimotor cortical areas and cerebellum. This observation underscores the contribution of somatosensory information to motor control related to grip force strength. Surprisingly, we did not find a similar pattern for basal ganglia networks despite their unique role in converting and integrating somatosensory information for guiding movements (Lidsky et al., 1985) and the abundant somatosensory cortex projections to the striatum (Flaherty & Graybiel, 1995). Along the same lines, we denote both similarities and subtle differences in the spatial distribution of networks defined by specific brain anatomy characteristics – morphometry and tissue properties. Given the co-localisation of myelin and iron related to oligodendrocyte myelination activity, we observe spatial overlap between networks defined by MT and R2* maps. Increasing the spatial granularity, the subtle differences in spatial distribution within basal ganglia and thalamus are consistent with the rostro-caudal distribution of iron in basal ganglia (Stüber et al., 2014) linked to a spatial gradient of dopamine receptor distribution (Rouault, 2013).

From a methodological point of view, our study contributes to extending the concept of structural covariance beyond the established morphometry features (Evans, 2013) that includes brain tissue properties (Accolla et al., 2014; Lorio et al., 2016; Melie-Garcia et al., 2018). The quantitative MRI approach provides complementary information to studies analysing functional and anatomical brain networks based on functional MRI in resting-state or diffusion-based tractography (Fox, 2018). Most importantly, building on the analytical framework of tissue property quantification rather than only on metrics derived from tissue class probabilities, we go beyond covariance analysis within a tissue class to show covariance of grey matter seeds with white matter areas and vice versa. This evidence lends not only credibility to the obtained findings, but it also represents a true multimodal network approach going beyond anatomical borders defined by the differential sensitivity of existing algorithms to the underlying MR contrast (Lorio et al., 2016).

We acknowledge several limitations that could potentially limit the generalisability of our findings. For the lesion data analysis, given the fact that lesion mapping was performed using a morphometric approach and T1-weighted MRI data, we cannot exclude that multi-parameter mapping of lesions could have resulted in a different spatial pattern of correlation with grip force, that would also lead to different covariance networks between specific tissue properties. Our ongoing studies using multi-parameter mapping in patients with stroke lesions will provide answers to this open question.

In summary, lesion network mapping combining structural covariance of volume and brain tissue properties delineates a cortico-subcortical circuitry associated with grip force control. Given the feasibility of analysing multiple MR contrasts across tissue boundaries, this approach provides complementary information to established network studies using diffusion-based tractography and functional connectivity metrics. A future extension should be the multi-variate analysis of the multi-contrast covariance networks, which could provide additional insight into the healthy and diseased brain.

Acknowledgments and Funding

We would like to thank all participants in the study. BD is supported by the Swiss National Science Foundation (NCCR Synapsy, project grant Nr. 32003B_135679, 32003B_159780, 324730_192755 and CRSK-3_190185) and the Leenaards Foundation. FK received funded from H2020-EU Morphemic project (Grant agreement ID: 871643). The CoLaus/PsyCoLaus study is supported by research grants from GlaxoSmithKline, the Faculty of Biology and Medicine of Lausanne, and the Swiss National Science Foundation (grants Nr. 3200B0_105993, 3200B0_118308, 33CSCO_122661, 33CS30_139468 and 33CS30_14840). LREN is very grateful to the Roger De Spoelberch and Partridge Foundations for their generous financial support. We thank Prof. Peter Vollenweider, Prof. Pedro Marques-Vidal and Prof. Gérard Waeber, Department of Medicine, Internal Medicine, CHUV, Lausanne, Switzerland, for their important contribution in the CoLaus/PsyCoLaus cohort recruitment.

Credit autor statement

Conception and design of the study: LW and BD.

Acquisition and analysis of data: LW, SF, LMG, MP, MLS, IS, FK, BD.

Drafting a significant portion of the manuscript or figures: LW, SF, LMG, MP, MLS, IS, FK, BD

References

Accolla, E.A., Dukart, J., Helms, G., Weiskopf, N., Kherif, F., Lutti, A., Chowdhury, R., Hetzer, S., Haynes, J.-D., Kühn, A.A., Draganski, B., 2014. Brain tissue properties differentiate between motor and limbic basal ganglia circuits. Hum. Brain Mapp. 35 (10), 5083–5092. doi:10.1002/hbm.22533.

Alexander-Bloch, A., Giedd, J.N., Bullmore, E., 2013. Imaging structural covariance between human brain regions. Nat. Rev. Neurosci. 14 (5), 322–336. doi:10.1038/nrn3465.

Alexander-Bloch, A., Raznahan, A., Bullmore, E., Giedd, J., 2013. The convergence of maturational change and structural covariance in human cortical networks. J. Neurosci. 33 (7), 2889–2899. doi:10.1523/JNEUROSCI.3554-12.2013.

Ashburner, J., 2007. A fast diffeomorphic image registration algorithm. Neuroimage 38 (1), 95–113. doi:10.1016/j.neuroimage.2007.07.007.

Burke, M.J., Joutsa, J., Cohen, A.L., Soussand, L., Cooke, D., Burstein, R., Fox, M.D., 2020. Mapping migraine to a common brain network. Brain 143 (2), 541–553. doi:10.1093/brain/awz405.

Carbonell, F., Bellec, P., Shmuel, A., 2014. Quantification of the impact of a confounding variable on functional connectivity confirms anti-correlated networks in the resting-state. Neuroimage 86, 343–353. doi:10.1016/j.neuroimage.2013.10.013.

Castella, R., Arn, L., Dupuis, E., Callaghan, M.F., Draganski, B., Lutti, A., 2018. Controlling motion artefact levels in MR images by suspending data acquisition during periods of head motion. Magn. Reson. Med. 80 (6), 2415–2426. doi:10.1002/mrm.27214.

Christopher, L., Koshimori, Y., Lang, A.E., Criaud, M., Strafella, A.P., 2014. Uncovering the role of the insula in non-motor symptoms of Parkinson's disease. Brain 137 (Pt 8), 2143–2154. doi:10.1093/brain/awu084.

Draganski, B., Ashburner, J., Hutton, C., Kherif, F., Frackowiak, R.S.J., Helms, G., Weiskopf, N, 2011. Regional specificity of MRI contrast parameter changes in normal ageing revealed by voxel-based quantification (VBQ). Neuroimage 55 (4), 1423–1434. doi:10.1016/j.neuroimage.2011.01.052.

Edelman, G.M., Gally, J.A., 2001. Degeneracy and complexity in biological systems. Proc. Natl. Acad. Sci. 98 (24), 13763–13768.

Evans, A.C., 2013. Networks of anatomical covariance. Neuroimage 80, 489–504. doi:10.1016/j.neuroimage.2013.05.054.

Firmann, M., Mayor, V., Vidal, P.M., Bochud, M., Pécoud, A., Hayoz, D., Paccaud, F., Preisig, M., Song, K.S., Yuan, X., Danoff, T.M., Stirnadel, H.A., Waterworth, D., Mooser, V., Waeber, G., Vollenweider, P., 2008. The CoLaus study: a population-based study to investigate the epidemiology and genetic determinants of cardiovascular risk factors and metabolic syndrome. BMC Cardiovascular Disord. 8 (1), 6. doi:10.1186/1471-2261-8-6.

Flaherty, A.W., Graybiel, A.M., 1995. Motor and somatosensory corticostriatal projection magnifications in the squirrel monkey. J. Neurophysiol. 74 (6), 2638–2648. doi:10.1152/jn.1995.74.6.2638.

Fox, M.D., 2018. Mapping symptoms to brain networks with the human connectome. N. Engl. J. Med. 379 (23), 2237–2245. doi:10.1056/NEJMra1706158.

Günther, C.M., Bürger, A., Rickert, M., Crispin, A., Schulz, C.U., 2008. Grip strength in healthy caucasian adults: reference values. J. Hand Surg. [Am] 33 (4), 558–565. doi:10.1016/j.jhsa.2008.01.008.

Helms, G., Dathe, H., Dechent, P., 2008. Quantitative FLASH MRI at 3T using a rational approximation of the Ernst equation. Magnet. Resonance Med. 59 (3), 667–672. doi:10.1002/mrm.21542.

Helms, G., Draganski, B., Frackowiak, R., Ashburner, J., Weiskopf, N., 2009. Improved segmentation of deep brain grey matter structures using magnetization transfer (MT) parameter maps. Neuroimage 47 (1), 194–198. doi:10.1016/j.neuroimage.2009.03.053.

Keisker, B., Hepp-Reymond, M.-C., Blickenstorfer, A., Meyer, M., Kollias, S.S., 2009. Differential force scaling of fine-graded power grip force in the sensorimotor network. Hum. Brain Mapp. 30 (8), 2453–2465. doi:10.1002/hbm.20676.

Kherif, F., Muller, S., 2020. Neuro-clinical signatures of language impairments: a theoretical framework for function-to-structure mapping in clinics. Curr. Top. Med. Chem. 20 (9), 800–811. doi:10.2174/1568026620666200302111130.

King, M., Rauch, H.G., Stein, D.J., Brooks, S.J., 2014. The handyman's brain: a neuroimaging meta-analysis describing the similarities and differences between grip type and pattern in humans. Neuroimage 102 (Pt 2), 923–937. doi:10.1016/j.neuroimage.2014.05.064.

Lidsky, T.I., Manetto, C., Schneider, J.S., 1985. A consideration of sensory factors involved in motor functions of the basal ganglia. Brain Res. Rev. 9 (2), 133–146. doi:10.1016/0165-0173(85)90010-4.

Lorio, S., Fresard, S., Adaszewski, S., Kherif, F., Chowdhury, R., Frackowiak, R.S., Ashburner, J., Helms, G., Weiskopf, N., Lutti, A., Draganski, B., 2016. New tissue priors for improved automated classification of subcortical brain structures on MRI. Neuroimage 130, 157–166. doi:10.1016/j.neuroimage.2016.01.062.

Lorio, Sara, Kherif, F., Ruef, A., Melie-Garcia, L., Frackowiak, R., Ashburner, J., Helms, G., Lutti, A., Draganski, B., 2016. Neurobiological origin of spurious brain morphological changes: a quantitative MRI study. Hum. Brain Mapp. 37 (5), 1801–1815. doi:10.1002/hbm.23137.

Melie-Garcia, L., Slater, D., Ruef, A., Sanabria-Diaz, G., Preisig, M., Kherif, F., Draganski, B., Lutti, A., 2018. Networks of myelin covariance. Hum. Brain Mapp. 39 (4), 1532–1554. doi:10.1002/hbm.23929.

Noppeney, U., Friston, K.J., Price, C.J., 2004. Degenerate neuronal systems sustaining cognitive functions. J. Anat. 205 (6), 433–442. https://doi/full/10.1111/j.0021-8782.2004.00343.x.

Pennati, G.V., Plantin, J., Carment, L., Roca, P., Baron, J., Pavlova, E., Borg, J., Lindberg, P.G., 2020. Recovery and prediction of dynamic precision grip force control after stroke. Stroke 51 (3), 944–951. doi:10.1161/STROKEAHA.119.026205.

Preibisch, C., Deichmann, R., 2009. Influence of RF spoiling on the stability and accuracy of T1 mapping based on spoiled FLASH with varying flip angles. Magn. Reson. Med. 61 (1), 125–135. doi:10.1002/mrm.21776.

Preisig, M., Waeber, G., Vollenweider, P., Bovet, P., Rothen, S., Vandeleur, C., Guex, P., Middleton, L., Waterworth, D., Mooser, V., Tozzi, F., Muglia, P., 2009. The PsyCoLaus study: methodology and characteristics of the sample of a population-based survey on psychiatric disorders and their association with genetic and cardiovascular risk factors. BMC Psychiatry 9, 9. doi:10.1186/1471-244X-9-9.

Prodoehl, J., Corcos, D.M., Vaillancourt, D.E., 2009. Basal ganglia mechanisms underlying precision grip force control. Neurosci. Biobehav. Rev. 33 (6), 900–908. doi:10.1016/j.neubiorev.2009.03.004.

Rondina, J.M., Park, C., Ward, N.S., 2017. Brain regions important for recovery after severe post-stroke upper limb paresis. J. Neurol. Neurosurg. Psychiatry 88 (9), 737–743. doi:10.1136/jnnp-2016-315030.

Rouault, T.A., 2013. Iron metabolism in the CNS: implications for neurodegenerative diseases. Nat. Rev. Neurosci. 14 (8), 551–564. doi:10.1038/nrn3453.

Seghier, M.L., Ramlackhansingh, A., Crinion, J., Leff, A.P., Price, C.J., 2008. Lesion identification using unified segmentation-normalisation models and fuzzy clustering. Neuroimage 41 (4), 1253–1266. doi:10.1016/j.neuroimage.2008.03.028.

Snider, S.B., Hsu, J., Darby, R.R., Cooke, D., Fischer, D., Cohen, A.L., Grafman, J.H., Fox, M.D., 2020. Cortical lesions causing loss of consciousness are anticorrelated with the dorsal brainstem. Hum. Brain Mapp. 41 (6), 1520–1531. doi:10.1002/hbm.24892.

Spraker, M.B., Yu, H., Corcos, D.M., Vaillancourt, D.E., 2007. Role of individual basal ganglia nuclei in force amplitude generation. J. Neurophysiol. 98 (2), 821–834. doi:10.1152/jn.00239.2007.

Sterr, A., Dean, P.J.A., Szameitat, A.J., Conforto, A.B., Shen, S, 2014. Corticospinal tract integrity and lesion volume play different roles in chronic hemiparesis and its improvement through motor practice. Neurorehabil. Neural Repair 28 (4), 335–343. doi:10.1177/1545968313510972.

Stüber, C., Morawski, M., Schäfer, A., Labadie, C., Wähnert, M., Leuze, C., Streicher, M., Barapatre, N., Reimann, K., Geyer, S., Spemann, D., Turner, R., 2014. Myelin and iron concentration in the human brain: a quantitative study of MRI contrast. Neuroimage 93, 95–106. doi:10.1016/j.neuroimage.2014.02.026.

Taubert, M., Roggenhofer, E., Melie-Garcia, L., Muller, S., Lehmann, N., Preisig, M., Vollenweider, P., Marques-Vidal, P., Lutti, A., Kherif, F., Draganski, B., 2020. Converging patterns of aging-associated brain volume loss and tissue microstructure differences. Neurobiol. Aging 88, 108–118. doi:10.1016/j.neurobiolaging.2020.01.006.

Ward, N.S., Newton, J.M., Swayne, O.B.C., Lee, L., Frackowiak, R.S.J., Thompson, A.J., Greenwood, R.J., Rothwell, J.C, 2007. The relationship between brain activity and peak grip force is modulated by corticospinal system integrity after subcortical stroke. Eur. J. Neurosci. 25 (6), 1865–1873. doi:10.1111/j.1460-9568.2007.05434.x.

Weiskopf, N., Suckling, J., Williams, G., Correia, M.M., Inkster, B., Tait, R., Ooi, C., Bullmore, E.T., Lutti, A., 2013. Quantitative multi-parameter mapping of R1, PD(*), MT, and R2(*) at 3T: a multi-center validation. Front. Neurosci. 7, 95. doi:10.3389/fnins.2013.00095.

Yee, Y., Fernandes, D.J., French, L., Ellegood, J., Cahill, L.S., Vousden, D.A., Spencer Noakes, L., Scholz, J., van Eede, M.C., Nieman, B.J., Sled, J.G., Lerch, J.P., 2018. Structural covariance of brain region volumes is associated with both structural connectivity and transcriptomic similarity. Neuroimage 179, 357–372. doi:10.1016/j.neuroimage.2018.05.028.